METEOROLOGICAL APPLICATIONS
Meteorol. Appl. **19**: 289–301 (2012)
Published online 6 May 2011 in Wiley Online Library
(wileyonlinelibrary.com) DOI: 10.1002/met.261

Crosswind thresholds supporting wake-vortex-free corridors for departing aircraft

K. Dengler,[a]* F. Holzäpfel,[a] T. Gerz,[a] A. Wiegele,[a] I. De Visscher,[b] G. Winckelmans,[b] L. Bricteux,[b] H. Fischer[c] and J. Konopka[c]

[a] *Deutsches Zentrum für Luft- und Raumfahrt (DLR), Institut für Physik der Atmosphäre, Oberpfaffenhofen, D-82234 Wessling, Germany*
[b] *Université catholique de Louvain (UCL), Institute of Mechanics, Materials and Civil Engineering (iMMC), B-1348 Louvain-la-Neuve, Belgium*
[c] *DFS Deutsche Flugsicherung GmbH, Research and Development, D-63225 Langen, Germany*

ABSTRACT: During two field measurement campaigns aircraft wake vortex trajectory and wind measurement data have been collected at Frankfurt airport. Three different approaches have been used to analyse the data in order to estimate crosswind threshold values supporting vortex-free corridors for departing aircraft. Although several competing effects such as wake vortex transport in and out of ground effect, temporal and spatial wind variability, and the spreading of aircraft trajectories after take-off, complicate the analyses, all three approaches lead to similar crosswind thresholds. Employing standard instrumentation at 10 m, a minimum crosswind threshold of 3.5–4.6 m s^{-1} has been identified to clear a safety corridor of 150 m width from wake vortices with a 95% probability within 60 s. Alternative estimations of crosswind thresholds employing different instrumentation and different height ranges are reported. Crosswind thresholds can be reduced if the wind is measured close to the air mass in which the vortices evolve. A definite crosswind threshold for operational use cannot be deduced solely from this study since critical factors such as risk and safety assessment have not yet been taken into account. Copyright © 2011 Royal Meteorological Society

KEY WORDS crosswind threshold; wake-vortex drift; aircraft separation; departure corridor; CREDOS

Received 24 September 2010; Revised 24 February 2011; Accepted 9 March 2011

1. Introduction

Counter-rotating wake vortex pairs shed by aircraft pose a potential risk on following aircraft in particular during approach and landing as well as take-off. In the 1970s aircraft weight dependent separation minima were introduced by the International Civil Aviation Organization (ICAO) to avoid hazardous wake vortex encounters. Following an EUROCONTROL study (2008) demand for air transport in 2030 is forecast to be about 1.8 times greater than in 2007 and airport capacity will lag the actual demand by 11%. The safe separations introduced by ICAO are considered to be over conservative under certain weather conditions (Frech and Zinner, 2004) opening the research for reduced separation and decreased delays during hours of peak demand.

The initial strength of the vortices is mainly determined by the weight, span and speed of the aircraft. The vortices descend due to mutually induced velocities. Wake vortex decay and descent strongly depend on the local meteorological conditions where the vortices evolve. Atmospheric turbulence, which may be characterized in terms of turbulent kinetic energy and/or eddy dissipation rate and vertical stability, characterized by the Brunt–Väisälä-frequency are key parameters influencing wake vortex decay. Vortex drift strongly depends on the ambient wind speed as well as the interaction with the ground at low altitude.

For a given crosswind speed the lateral vortex drift can be calculated theoretically. In practice several mechanisms may cause significant deviations from this theoretical drift speed (Holzäpfel, 2003; Rossow *et al.*, 2005). First of all, the atmospheric boundary layer is turbulent: the wind speed is not constant in space and time. Second, the vortices themselves do not remain straight vortex tubes but may deform substantially. When, finally, vortex rings have formed (Crow, 1970) the lateral vortex dimensions may reach up to more than five times their initial spacing (Hennemann, 2009). Vortex interaction with wind shear may cause vortex tilting and lateral vortex drift (Meleshko *et al.*, 2001). There is also an indirect impact of the vortex descent speed on lateral vortex transport. Varying vortex descent speeds along vertical crosswind profiles lead to different lateral transport distances. Finally, when approaching the ground the vortices first diverge along hyperbolic trajectories, then secondary vortices detach from the boundary layer at the ground causing the wake vortices to rebound and decay strongly (see e.g., Winckelmans *et al.*, 2006; Holzäpfel and Steen, 2007).

Most of the studies so far have focused on aircraft approach and landing (for a comprehensive summary, see Elsenaar, 2006). Within the European Union (EU) project

* Correspondence to: K. Dengler, Deutsches Zentrum für Luft- und Raumfahrt, Institut für Physik der Atmosphäre, Oberpfaffenhofen, D-82234 Wessling, Germany. E-mail: klaus.dengler@dlr.de

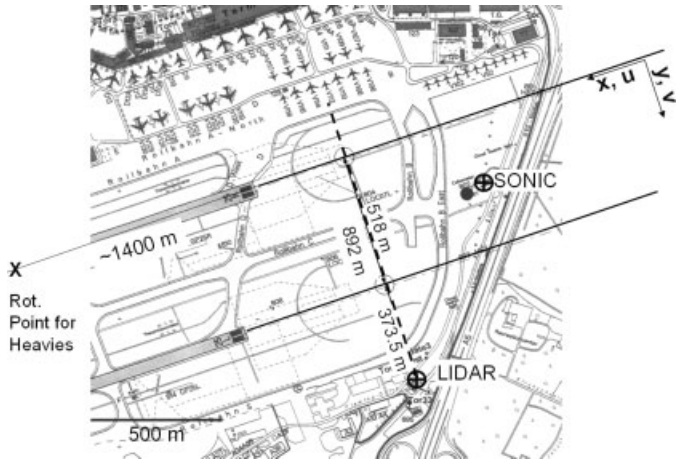

Figure 1. Location of sensors and measurement planes within the EDDF-1 campaign including the orientation of the employed coordinate system and the rotation point of heavy aircraft. Flight direction is in easterly direction. Local Operation Centre, LOZ [●], Sites of DLR Lidar and SONIC [⊕], Intersection of glide path with Lidar beam [◯].

CREDOS (Crosswind Reduced Separations for Departure Operations, 2006–2009) the operational feasibility of reduced wake turbulence separation for departing aircraft under certain crosswind conditions has been studied. Within this project two measurement campaigns for wake vortices generated by departing aircraft at Frankfurt airport have been carried out. One of the project's objectives was to identify crosswind situations that ensure rapid transport of the vortices out of the flight corridor and thus to allow for conditional reduction of the separation time between departing aircraft from currently 120 s (ICAO) to 90 or 60 s.

The current investigation is based on the two data sets gathered at Frankfurt Airport which will be described in detail in Section 2. In Section 3, three different approaches to estimate crosswind thresholds for different aircraft separation times are presented and the results obtained are discussed in Section 4, followed by some conclusions in Section 5. Note that the conducted analysis is not suited to quantify the related risks and to set the risks in relation to the ICAO reference scenario. The complete analyses can be found in the CREDOS project reports (see Konopka and Fisher, 2008; De Visscher *et al*., 2009).

2. Measurement setup and data description

The analyses of crosswind transport of wake vortices presented in this paper employ the data of two field measurement campaigns conducted at Frankfurt Airport (EDDF) in 2006 and 2007.

2.1. EDDF-1 campaign

During the measurement period of EDDF-1 between 21 December 2006 and 28 February 2007, 147 wake vortex pairs of heavy aircraft departures were measured, where the majority of the vortices developed out of ground effect. All departures were on runway 07 to the east. The 2 μm pulsed Lidar system (a Wind Tracer of Lockheed Martin Coherent Technology) of the Deutsche Zentrum für Luft- und Raumfahrt (DLR) was located close to the da Vinci house in the southeast edge of the terminal area (Figure 1).

For departures on runway 07L, the Lidar was used for vortex characterization. For this purpose the Lidar scanned perpendicular to the flight direction and collected vortices generated in a height range from 100 to 400 m. For the evaluation of wake-vortex properties, an interactive four-stage data processing algorithm was applied (Köpp *et al*., 2004). In that study first profiles of vortex tangential velocities were estimated, from which vortex positions and circulations were derived. The error for vortex core position was determined to about 4.5 m in the vertical and 6.5 m in the horizontal directions and to 13 $m^2\ s^{-1}$ for circulation (Köpp *et al*., 2005). Because of non-optimal meteorological measurement conditions during the present campaign (very strong winds and relatively poor signal to noise ratios) the error in circulation is expected to be slightly higher in the present dataset.

In addition, a sonic anemometer with a sampling frequency of 20 Hz provided measurements of wind and turbulence at 10 m. For the determination of crosswind thresholds the current study employs 10 m measurements because these are available at airports operationally.

2.2. EDDF-2 campaign

A second measurement campaign, the EDDF-2 campaign, took place during a 6 month period between January and June 2007. The EDDF-2 campaign aimed at the generation of a large, statistically meaningful sample of wake trajectories generated by heavy aircraft shortly after lift off and the characterization of these events in the full operational and meteorological context. To do so, significant automation and integration of data collection, quality assurance and data fusion procedures had to be employed. In particular, an interactive data processing

as with the much smaller EDDF-1 data sample was not feasible.

Wake vortex trajectories (lateral and vertical wake positions) and circulation data have been collected with an FAA-owned WindTracer Doppler Lidar which was operated by DFS during the EDDF-2 campaign. As in EDDF-1 the wake vortices have been observed in a single cross-plane of the initial take-off path of the aircraft, whilst neglecting the influence of the wind component parallel to the runway on the age of a vortex.

After an analysis of the heavy aircraft's rotation points and consideration of the sitting requirements including, e.g.:

- accessibility and security;
- availability of electric power supply and communication infrastructure;
- the necessity of having an unobstructed line of sight for the laser beam, and
- the optimum operating range of the Lidar.

An area next to the General Aviation Apron south of the parallel runways 25R and 25L was selected (Figure 2).

In parallel to the wake vortex measurements radar track data have been collected for determination of the wake generating aircraft type and characterization of the initial aircraft trajectories in terms of rotation point, climb angles and airspeed. In the context of this paper it is important to note that the onset of the evolution of the vortices (vortex age = 0) is determined by the aircraft intersecting the Lidar scan plane as it was computed from the aircraft trajectories.

The meteorological situation is characterized by various sensors at different locations (Figure 2 and Konopka and Fischer, 2007, for a complete description):

- surface wind from standard instrumentation at 10 m above ground (such instrumentation is available on any airport siting and the measurement is according to the standards set out in ICAO Annex 3, 2004). That is, the anemometers are not situated in close proximity to the wake measurement site and are thus representing an operational approach avoiding additional costs for dedicated wind measurement devices;
- a Wind-Temperature Radar (WTR) supplemented by a Radio Acoustic Sounding System (RASS). The WTR/RASS provides wind, temperature and turbulence profiles within the height range of 60–1650 m with 30 m vertical resolution (Konopka and Fischer, 2005), and
- a WindTracer Doppler Lidar system that provides lateral and vertical wake vortex positions and circulation values. The WindTracer's optimum range for wake tracking is roughly between 400 and 2000 m. Also, Lidar-measured crosswind profiles for heights between 1.65 and 190 m are evaluated.

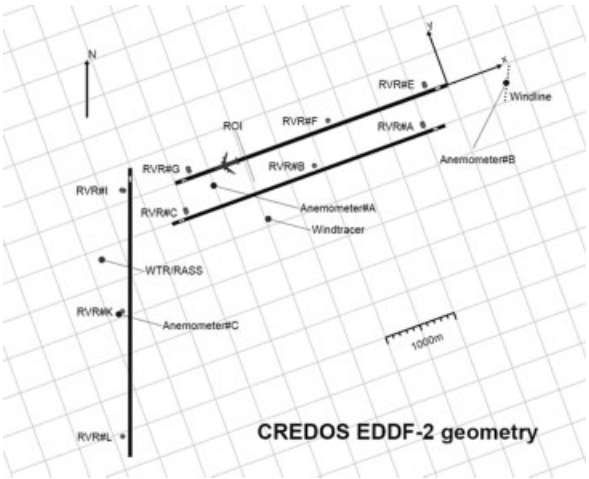

Figure 2. Coordinate system and sensor sites of the EDDF-2 campaign.

The EDDF-2 database contains a total of 10 442 wake vortex cases generated by heavy and medium aircraft taking off to the east in a height range from near ground up to 150 m. Due to the low altitude most of the vortices developed in ground effect (IGE). The large sample generated by an automatic data evaluation procedure and the wide range of meteorological conditions in this database enables well-converged statistical analyses to be performed.

3. Three approaches to estimate crosswind thresholds

Correlation of crosswind data taken with different instruments with wake vortex trajectory data gathered by the Lidar was used to determine the minimum required crosswind to assure that wake vortices have cleared a specified flight corridor with a certain probability within a defined time interval after take-off. The initial age (age = 0) is defined as the time when the aircraft intersects the Lidar scan plane. Ultimately, the identified time intervals could be translated into aircraft separation times once all other requirements prerequisite to the installation of a crosswind based wake-vortex system are met.

EDDF-1 data have been analysed by Deutsches Zentrum für Luft- und Raumfahrt (DLR) to study wake vortex transport out of ground effect (approach 1), while the EDDF-2 database where the majority of the vortices developed in ground proximity has been analysed by Université catholique de Louvain (UCL, approach 2) and Deutsche Flugsicherung (DFS, approach 3). Different assumptions regarding level of probability, corridor size and crosswind computation are used by these approaches when analysing the data. However, the different analyses for similar assumptions were also compared. Crosswind data from different instrumentation and different height ranges are employed. However, the paper focuses on wind data measured at 10 m height as this altitude is used by default for airport operations. The different approaches will now be described in detail.

3.1. Approach 1: computation based on sonic anemometer wind measurements using the EDDF-1 database

During 7 days of Lidar measurements 147 departures of heavy aircraft have been measured. The measurements confirm that vortex behaviour and displacement strongly depend on meteorological conditions. A distinct correlation of crosswinds with horizontal displacement of the vortices was observed. The period in which the vortices could be observed was limited during the measuring days in January because the vortices were displaced out of the measurement range by the strong crosswind before they dissipated. As expected, all of the vortex pairs are descending with time.

First, the distance that wake vortices have to be displaced laterally to clear the area of concern was determined. In contrast to the approach phase where the adherence to the Instrument Landing System (ILS) limits aircraft deviations a definition of a safety corridor for departing aircraft is more arbitrary. This is due to the different rotation points and varying climb rates of the various aircraft types.

Besides the definition of a corridor half width of 100 m, which allows for the comparison to the other approaches in Sections 3.2 and 3.3 a corridor width from the distribution of lateral aircraft positions within the Lidar observation plane is estimated. Only for this purpose and to avoid artificial increase of the flight corridor caused by vortex drift the initial (y, z)-positions (with y perpendicular to the runway and z being the vertical axis) of the wake vortices were extrapolated to the time of vortex generation and the resulting distributions were fitted by Gaussian distributions. The required clearance distance is then calculated as the sum of the mean vortex spacing ($b_0 = 50.6$ m) plus two times the 2σ-value (95%) of the estimated distribution of lateral aircraft positions ($\Delta_{ac} = 49.0$ m). The resulting corridor half width:

$$d = \frac{1}{2}(b_0 + 2\Delta_{ac}) \tag{1}$$

amounts to roughly 75 m. The first line of Table I summarizes the required drift velocities needed to clear the flight corridor for different aircraft separation times by using $v_{req} = \frac{2d}{t_{sep}}$ with t_{sep} being the aircraft separation time. Additional safety distances between vortex centre and follower aircraft (Schwarz and Hahn, 2006) are not considered in this study.

Table I. Drift velocities obtained by approach 1 needed to displace the vortices by 150 m for given aircraft separation times.

Clearance time (s)	50	60	90	120
v_{req} (m s^{-1}) for clearance	3.0	2.5	1.67	1.25
u_c (m s^{-1})	4.1	3.7	3.1	2.8

Crosswind velocities at 10 m height needed for clearance of aircraft corridor employing a 95% probability.

The measured vortex drift velocities show considerable variation due to e.g. effects of turbulence and vortex deformation. The mean observed wake vortex drift speed, v_{drift} is calculated from the Lidar data through:

$$v_{drift} = \frac{y_{initial} - y_{last}}{t_{initial} - t_{last}} \tag{2}$$

where $y_{initial}$ is the initial vortex position at the first time of detection $t_{initial}$, y_{last} denotes the vortex position at the time of last measurement t_{last}. The larger the times and distances the more accurate the calculated average vortex drift speed.

A linear approach was used to estimate the crosswind thresholds needed to clear the $2d = 150$ m corridor. Only luff vortices are considered since those have to drift a longer distance to leave the corridor. In the coordinate system used (Figure 1) and the take-off direction to be east, the left (right) vortex is the luff vortex if the crosswind is positive (negative).

Figure 3 shows the observed vortex drift velocity of the luff vortices depending on the crosswind measured at 10 m above ground including a linear fit and the respective 95% envelopes. The calculated drift velocity of each measured vortex is represented by a single data point. The linear fit allows deriving a relation between the 10 m crosswind and the resulting mean vortex drift velocity. Based on the lower 95% envelope of the vortex drift velocity v_{drift} a crosswind threshold u_c can be determined which assures the advection of 95% of the vortices out of the flight corridor. The aircraft separation time specifies the required vortex drift velocity, v_{req}, to clear a certain corridor from wake vortices. The resulting crosswind threshold fit can then be calculated according to:

$$u_c = \frac{v_{req} + 2.68 \text{ m s}^{-1}}{1.39} \tag{3}$$

The crosswind thresholds needed to clear a corridor with half width of 75 m from wake vortices for different

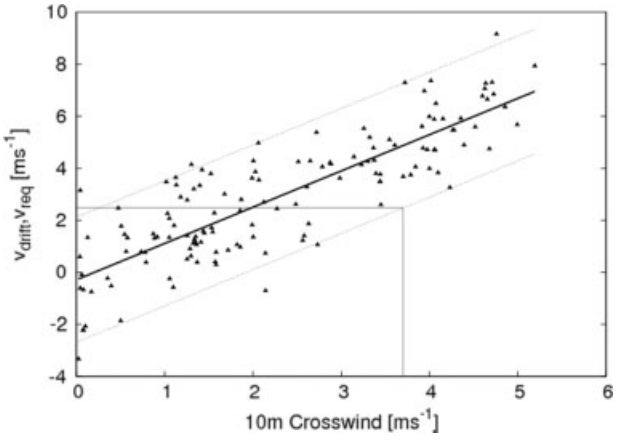

Figure 3. Drift speed v_{drift}, required vortex speed, v_{req} of upwind (luff) vortices (triangles) and crosswind at 10 m height measured by the SONIC. The linear fit is shown by the solid line surrounded by the 95% envelopes (dotted lines). The horizontal and vertical lines explain the use to estimate a crosswind threshold for a 60 s separation (see text).

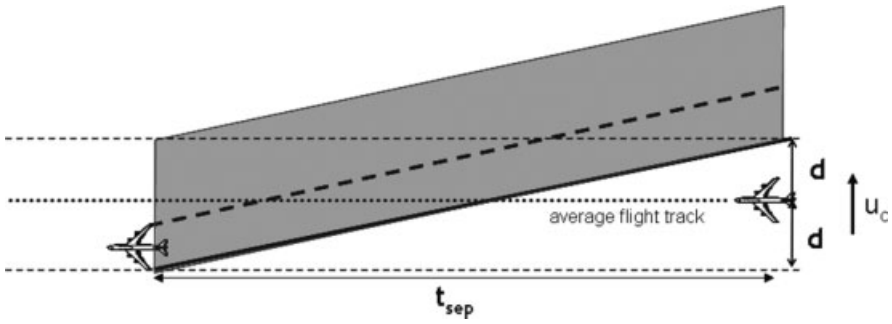

Figure 4. Schematic illustration of approach 1. The grey shaded area shows the corridor of the leading aircraft which includes the wake vortices with a 95% probability level. Leading and following aircraft with defined separation time t_{sep}, average flight track and direction of crosswind are indicated. The dashed and solid thick lines starting at the wing tips of the leading a/c indicate exemplary positions of the wake vortices.

aircraft separation times according to Equation (3) are listed in Table I (second line). In Figure 3 the method is illustrated exemplarily: assuming a separation time of 60 s a required vortex drift speed of 2.5 m s^{-1} is needed (Table I). Following the horizontal line in Figure 3 to the intersection with the lower boundary of the 95% envelope a crosswind threshold of 3.7 m s^{-1} needed to clear the flight corridor on a 95% probability is obtained.

The same analysis was done without distinguishing between luff and lee vortices meaning that all vortices were used for the linear fit. The crosswind thresholds obtained were only about 0.1 m s^{-1} lower which is negligible. This result is not unexpected since the vortices measured within EDDF-1 developed at altitudes where no ground effects were observed that could influence the luff and lee vortices in different ways.

Figure 4 gives a schematic illustration of this approach. The wake vortices shed by the leading aircraft can be found within the grey shaded area with a probability of 95%. This area is advected from the average flight track by the crosswind. The position of the leading aircraft shown is the extreme situation where the luff vortices are generated at the upwind edge of the area of interest. For a given separation time t_{sep} the described approach then results in a crosswind threshold needed for the following aircraft to avoid wake vortex encounters. The described method is in principle applicable to any flight level above b_0 since all wake vortices used in the analysis developed out of ground effect. This is the key difference to the other approaches described next.

The probability of not encountering the vortices is actually much higher than 95% because firstly only the missing 2.5% on one side of the symmetric distribution is critical (the 2.5% on the other side correspond to vortices that have moved farthest from the centreline) and secondly, on average, the leading heavy aircraft take off late and climb slowly whereas the following medium weight class aircraft take off early with a steep climb rate. Thereby, the respective flight tracks are well separated. Additionally, wake vortex descent increases the vertical separations between the vortices and the follower aircraft.

3.2. Approach 2: computation based on Lidar wind measurements using the EDDF-2 database

During the 6 months of the EDDF-2 measurement campaign, 10 442 cases of tracked vortices have been collected. Since this database is very large it was first screened using well-defined criteria in order to retain 6950 cases which are considered relevant for further analysis. Cases for which only one of the two vortices was measured were excluded. Cases with a too low or too high initial measured vortex spacing and bank angle were also discarded. Finally, the WindTracer algorithm used to compute the circulation does not calculate circulation values above ~750 m^2 s^{-1}. For larger values the algorithm sets the circulation data to exactly 800 m s^{-1} (Section 3.3). Since this is an arbitrary limit of the algorithm, those cases were also excluded.

Next, the wake vortex lateral transport has been correlated with the crosswind u_c using three different definitions of the crosswind measured by the Lidar:

- the crosswind measured at 10 m, $u_c(h = 10\ \text{m})$;
- the averaged crosswind from 0 to 100 m altitude; $u_{c,mean}$, and;
- the crosswind measured at the mean altitude of the measured vortices, $u_c(h_{mean})$.

Figure 5 shows a schematic view of the different crosswind definitions. The present study mainly focuses on the crosswind measured at 10 m with the Lidar.

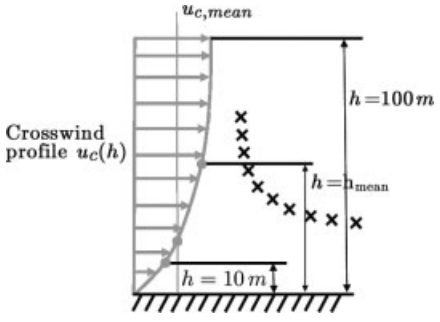

Figure 5. Schematic description of the crosswind velocities. The black crosses indicate the port vortex trajectory. The bullets indicate the three crosswind definitions used in approach 2.

This height has also been used in the two other data analyses approaches described here. It is worth noticing that the Lidar measures the wind exactly within the plane where the measured vortices evolve. It is thus the best measurement of the wind as experienced by the vortices. Consequently, for an anemometer at some further distant location the crosswind will deviate more from the crosswind sensed by the vortices and the resulting crosswind thresholds will be somewhat higher.

For five vortex ages, from 40 to 120 s, and for each individual departure, the net lateral displacement of the vortices, $\Delta y = y_{\text{last}} - y_{\text{initial}}$, is correlated to the measured crosswind u_c. From the 13 900 measured vortices (6950 vortex pairs), one computes, for each vortex age, the mean correlation coefficient α between displacement and crosswind and the envelopes containing 90, 95, and 99% of the measurements. The linear fit used on the data points for respectively the upwind, the downwind and both vortices, is then given by Equation (4):

$$\Delta y(u_c, t) = \alpha \times u_c t \tag{4}$$

Figure 6 presents the correlation between $u_c(h = 10\text{ m})$ and Δy of all vortices for a vortex age of 60 s. The mean behaviour and the 95% envelope are also shown. The values of the fit parameters for the different times are provided in Table II. The mean value of $\alpha = 1.15$ indicates that the lateral transport of the wake vortices (both due to wind and ground effects) is on average 15% higher than the crosswind measured at 10 m height. Without wind the left and right vortices move a finite distance due to ground effect. If left and right vortices are averaged the net displacement is zero.

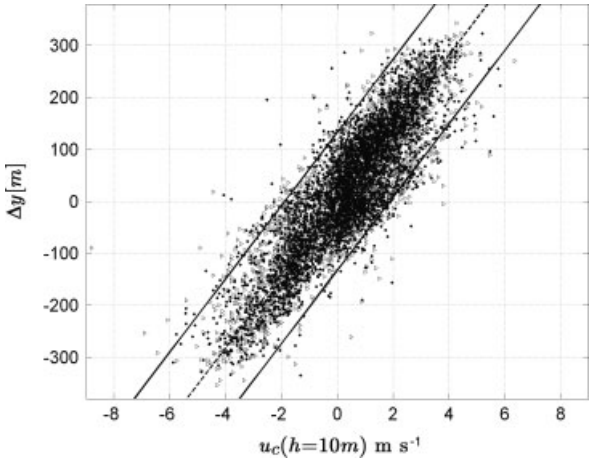

Figure 6. Evolution of the vortex net lateral displacement as a function of the crosswind u_c at 10 m for a time separation of 60 s. The triangles (resp. the dots) show the displacement of the starboard (resp. the port) vortices. A linear fit shows the mean evolution (dashed line). The envelope containing 95% of the total examined vortices is denoted by solid lines. Six thousand and nine hundred and fifty measured vortex pairs are used.

Table II. Averages of α parameter of the linear fit of approach 2, Equation (4), for the different vortex ages.

t_{sep} (s)	40	60	80	100	120	AVG
α	1.24	1.17	1.13	1.07	0.98	1.15

A slow decrease of the α factor with time is observed. This behaviour can be explained by considering three steps. In the first step, the vortices are not IGE yet and sink progressively. Assuming a typical wind profile, the crosswind experienced by the vortices is initially higher than the crosswind at 10 m height and decreases as the vortices sink. The α value decreases thus accordingly. In the second step, the vortices are IGE and interact with the secondary vorticity generated at the ground. With crosswind, the upwind (resp. downwind) vortex travels slower (resp. faster) than the wind. The average displacement speed of the down- and upwind vortices is slightly smaller than the local wind speed. Finally, in the third step, the vortices rebound and move again with the local wind speed. Since the α factor represents an accumulated effect of the wind on the vortex displacement after a certain time, it is to be expected to observe a slow decrease of α until it reaches a plateau.

Moreover, the (90, 95 or 99%) envelope half width, W, is seen to grow linearly in time, at least for the time window of interest. A linear fit is thus also used for W given by Equation (5):

$$W(t) = \frac{dW}{dt} t + W_0 \tag{5}$$

According to this database analysis, after a certain time t, the wake vortices, experiencing a crosswind u_c, would have travelled a net lateral distance Δy comprised of the interval:

$$\Delta y \in \left[\left(\alpha u_c - \frac{dW}{dt} \right) t - W_0, \left(\alpha u_c + \frac{dW}{dt} \right) t + W_0 \right]. \tag{6}$$

One can thus compute the crosswind needed for the vortices to travel a certain distance within a certain time when using the prescribed envelopes (respectively 90, 95 and 99%). Alternatively, one can compute, for a given crosswind value, the time needed for the vortices to travel a certain distance.

Likewise, one can compute the crosswind threshold needed for the vortices to be at least at a distance d from the runway centreline after a time t_{sep}. Figure 7 shows a schematic view of the use of such envelopes. In this figure, for graphical purpose, the envelopes are extrapolated for time separations shorter than 40 s. However, the envelopes were built and are used for times between 40 and 120 s. The obtained crosswind thresholds are reported in Table III, for three aircraft separations and three corridor half widths d. Two additional corridor half widths defined by $d_1 = 0.5^* \times$ runway width + wingspan $\approx$100 m and $d_2 =$ wingspan $\approx$ 50 m have been included in Table III. The study has been performed separately considering the wake vortices generated by medium aircraft, by heavy aircraft and by the combination of

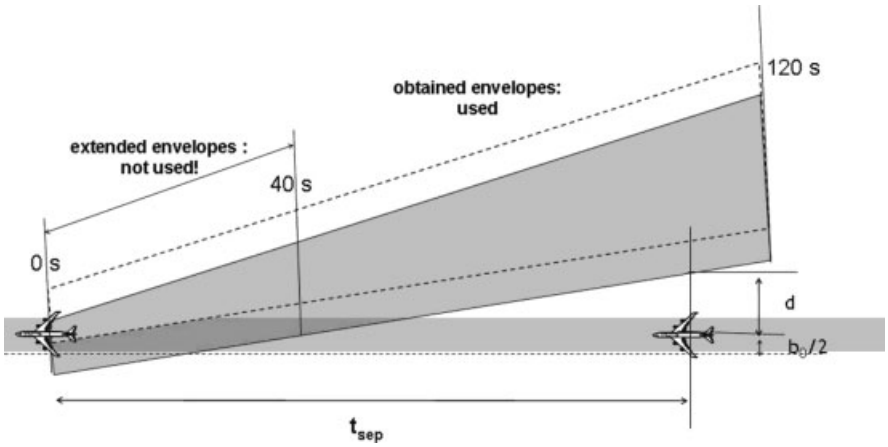

Figure 7. Schematic illustration of approach 2. The solid envelope contains the port vortices while the dashed envelope contains the starboard vortices. The envelopes have been extended to times below 40 s but, at these times, the results are not used.

Table III. Crosswind $u_c(h = 10\ \text{m})$ in m s^{-1} obtained by approach 2 and needed to move the WV generated by medium (top), heavy (middle) and all aircraft (bottom) respectively 50, 75 and 100 m away from the runway centreline when using the 95% probability envelopes.

t_{sep} (s)	50 m	75 m	100 m
		Medium	
60	2.6	3.0	3.3
90	2.1	2.4	2.6
120	1.9	2.1	2.2
		Heavy	
60	3.1	3.5	3.9
90	2.4	2.6	2.9
120	2.0	2.2	2.4
		All	
60	3.0	3.4	3.7
90	2.3	2.6	2.8
120	2.0	2.2	2.4

both. For instance, using the 95% envelope, a crosswind $u_c(h = 10\ \text{m}) = 3.5\ \text{m s}^{-1}$ is required for the vortices, generated by heavy aircraft, to be at least at a distance $d = 75$ m from the runway centreline for an aircraft separation of 60 s.

Further, Table III indicates that the crosswind thresholds for the heavy aircraft are consistently higher or at least equal to those of the medium aircraft. This is related to the fact that wake vortices of the heavies were mostly measured IGE. The ground effect tends to reduce the lateral transport of the upwind vortex and to increase the lateral transport of the downwind vortex. In the Lidar scan plane, the vortices, generated by heavy aircraft, were on average lower because those aircraft rotate, on average, later and climb less steep. Moreover, the height at which the ground effect starts to play a role depends on the vortex separation b_0. Since the wing span, and thus b_0, is higher for heavy aircraft, the vortices shed by those aircraft enter in ground effect at higher altitudes than those generated by medium aircraft. In the database, more vortices generated by heavy aircraft are IGE than those generated by medium aircraft.

Finally, this analysis highlights also the benefits of using a more sophisticated definition of the crosswind than $u_c(h = 10\ \text{m})$. In that respect, the crosswind averaged over the first 100 m, $u_{c,mean}$, is of special interest as it is still operationally feasible and can be obtained, for instance, by a Lidar or a SODAR/RASS instrument installed at the airport. Using the 95% envelope, a crosswind $u_{c,mean} = 3.9\ \text{m s}^{-1}$ is required for the vortices, generated by heavy aircraft, to be at least at a distance $d = 75$ m from the runway centreline for an aircraft separation of 60 s. It is important to stress that, due to the wind profile shape, the altitude-averaged wind, $u_{c,mean}$, is on average 17% higher than the 10 m height crosswind (see scheme in Figure 5). This ratio has been established based on the EDDF-2 measurements and is also verified to be consistent with the typical turbulent wind profile (i.e. using the logarithmic profile which is valid up to 100 m). Thus, an altitude-averaged crosswind $u_{c,mean} = 3.9\ \text{m s}^{-1}$ corresponds to a 10 m height crosswind $u_c(h = 10\ \text{m}) = 3.3\ \text{m s}^{-1}$. Operationally, for the same wind conditions, the wind threshold to be used will be lower when using a more sophisticated wind measurement since it best represents the wind as experienced by the vortices.

3.3. Approach 3: computation based on WTR/RASS, sonic anemometer and Lidar wind measurements using the EDDF-2 database

Similar to the previous analysis different crosswind definitions are used:

- crosswind measured at 10 m height with any of the anemometers displayed in Figure 2;
- the crosswind average between 60 and 200 m as determined by WTR/RASS;

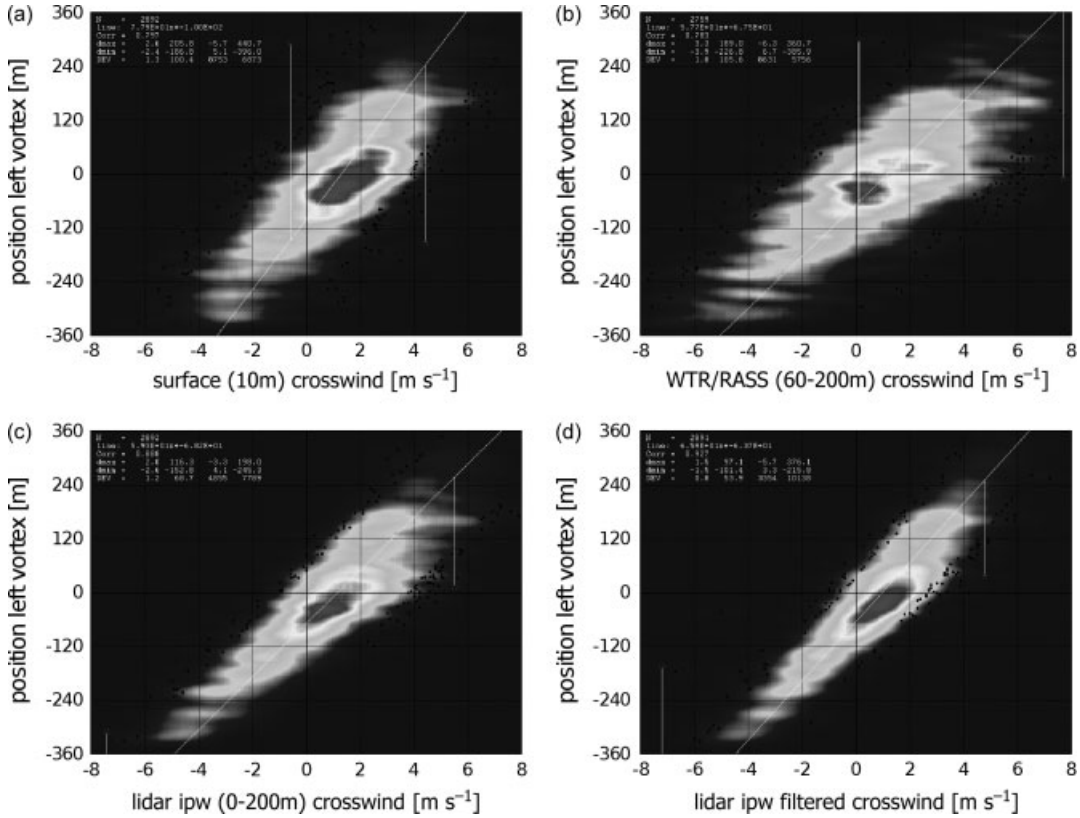

Figure 8. Vortex position versus crosswind contours for different methods to measure crosswind: (a) Crosswind at 10 m, (b) mean crosswind from WTR between 60 and 200 m, (c) averaged in-plane wind between 0 and 200 m measured by the Lidar and (d) filtered in-plane Lidar wind restricted to the altitude where the vortices evolve.

- the average in-plane wind between 0 and 200 m as measured by the Lidar, and,
- the average in-plane wind from the Lidar restricted to the altitude where the vortices evolved.

Recall that the Lidar is scanning in a cross-plane of the runway centreline, thus in-plane wind is almost equal to the crosswind. A small difference arises from the fact that the lidar beam is scanning and generally not measuring parallel to the surface. For the setup used in EDDF-2 and the highest measurement altitude this error is 2% of the crosswind in 200 m above ground disregarding the contribution of vertical wind speeds. This error is neglected as well as the fact that the Lidar measurement involves effectively a weighted average over a distance on the order of the laser pulse length.

The correlation of crosswind with vortex transport is quantified by the following procedure: for any of the vortices the lateral (y-coordinate) position at a given vortex age has been combined with a crosswind for this very event. Hereby, vortices from heavy aircraft and medium aircraft are analysed in separate classes as well as left and right vortices are analysed independently from each other. Vortex ages of 0, 20, 40, 60, 80, 100 and 120 s have been chosen. In that manner 112 different sets of vortex position and crosswind pairs have been obtained.

An example of such sets showing the effect of the different methods to determine crosswind is given in Figure 8. Figure 8 depicts the lateral distributions of the left vortices of heavy aircraft 60 s after generation. It can be seen immediately that the various methods of measuring crosswind do have an impact on the observed distributions of vortex displacement at a given crosswind. Obviously, the best correlation between vortex transport and crosswind is achieved when the wind is measured close to the air mass which actually advects the vortices (filtered in-plane Lidar).

For any of the 112 different sets of crosswind and vortex position pairs some parameters characterizing the distribution have been computed:

- the number of cases contributing to the set under consideration;
- a least squares straight line has been fitted through the data points; for this line:
  - the position offset, i.e. the value of the regression line at zero crosswind, and,
  - its slope have been determined;
- the correlation coefficient between crosswind and lateral position and
- the minimum (maximum) crosswind required to ensure that only a 2.5% fraction (corresponding to roughly the 2σ boundary for a normal distribution) of the leftmost (rightmost) vortices remain within a corridor (d) of 50 or 100 m to either side of the runway centreline.

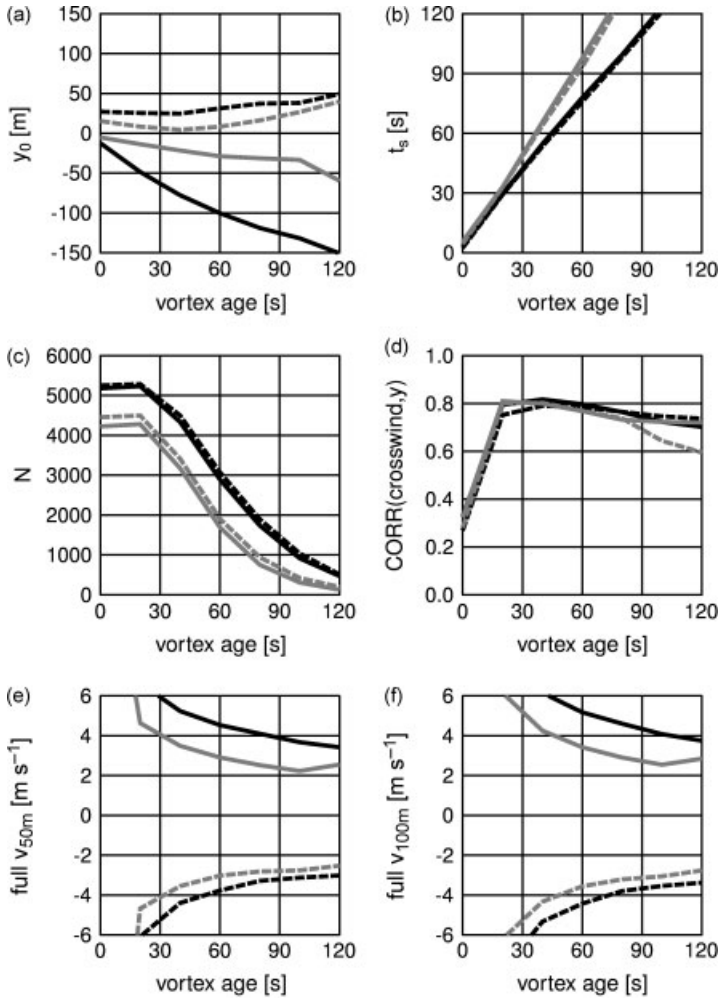

Figure 9. Parameters characterizing the relation between lateral vortex transport and surface crosswind at 10 m height: (a) offset, (b) slope, (c) number, (d) correlation, (e) 2.5% within ±50 m and (f) 2.5% within ±100 m. Properties of heavy aircraft vortices' are shown as black lines, those of medium aircraft vortices as grey lines. Right vortices are shown as full lines, left vortices as dashed lines. Heavy aircraft, left vortex [▬], heavy aircraft, right vortex [▬ ▬], medium aircraft, left vortex [▬], medium aircraft, right vortex [▬ ▬].

Before discussing the results for the different methods to measure crosswind in more detail, the working hypotheses are summarized:

- there should be a mirror symmetry in the behaviour of left and right vortices;
- in this experimental setup, ground effect should have less of an impact on medium aircraft vortices (since they are less frequent and shorter in ground effect) than on heavy aircraft;
- ground effect is independent of crosswind and
- the slope should equal vortex age; a wind of speed u impacting on the vortices for a time t should transport the vortices the distance $u \times t$; note that ground effect becomes manifest in the slope changing with time (= vortex age).

Figure 9 shows the characteristic parameters when the surface measurement is used as the characteristic crosswind. In the case of surface wind as a means to determine crosswind, the offset (Figure 9(a)) is not showing the expected symmetry. The slope (Figure 9(b)) is exceeding the vortex age considerably and it is different for heavy and medium aircraft. Correlation (Figure 9(d)) is hardly exceeding 0.8. Note that the percentiles are related to the number of vortices observed at the given age t (Figure 9(c)). Figures 9(e) and (f) show crosswind thresholds with different widths of the corridor. The asymmetry of the offset, which is most pronounced in Figure 9(a) is due to the fact that the crosswind has been measured at different altitude and some distant location from where the vortices evolved. Since the vortices move at altitudes considerably higher than 10 m, where the wind is measured, this asymmetry may also result from the Ekman spiral, i.e. the change of wind direction with altitude in the atmospheric boundary layer. This asymmetry will be different at other airports or runways. In order to simplify the results, crosswind thresholds are symmetrized, i.e. only the maximum of the absolute values of the respective thresholds for left and right vortices are listed in Table IV.

Symmetry in the offset, the slope and correlation are improving when crosswinds at higher altitudes are included. Figure 10 shows that these indicators improve

Table IV. Crosswind thresholds for surface wind measurements at 10 m height estimated by approach 3.

t_{sep} (s)	Medium			Heavy		
	50 (m)	75 (m)	100 (m)	50 (m)	75 (m)	100 (m)
40	3.6	4.0	4.4	5.0	5.4	5.9
60	3.1	3.4	3.6	4.3	4.6	5.0
80	2.9	3.0	3.2	4.0	4.2	4.5
100	2.5	2.7	2.9	3.6	3.8	4.0
120	2.4	2.6	2.7	3.5	3.6	3.8

The crosswind threshold is given for various combinations of vortex age t (equal to t_{sep}) and corridor half-width d and for heavy and medium aircraft separately. The unit is m s^{-1}, a 95% probability is assumed.

even further, when the crosswind as measured by the WindTracer is used and in particular when the crosswind is averaged only in the height band where the vortices have evolved. However, at the present stage these additional crosswind definitions are not used in airport operations.

To analyse the asymmetry between the right and left vortex the vortex motion in ground effect is discussed briefly for heavy aircraft. For any two consecutive observations of the same vortex a vortex lateral speed has been computed. The vortex self induced speed is yield after subtraction of the crosswind, here taken from the WindTracer in-plane wind profile. Taking into account the error of the vortex position measurement and considering the potentially amplifying effect of the numerical differentiation involved, a considerable statistical error can be expected.

Again, the technique to superimpose a large number of such data points with relatively large error was employed to obtain an estimate of the average behaviour with much smaller error than the single measurement. The vortices' self-induced speed as a function of altitude in non-dimensional form is shown in Figure 11. These plots represent more than 100 000 data points. Above one wingspan, b, the distributions are symmetric, suggesting that there is no effect of ground vicinity. Below half a wingspan, the ground effect shifts the right vortices' distributions towards positive velocities and likewise the left

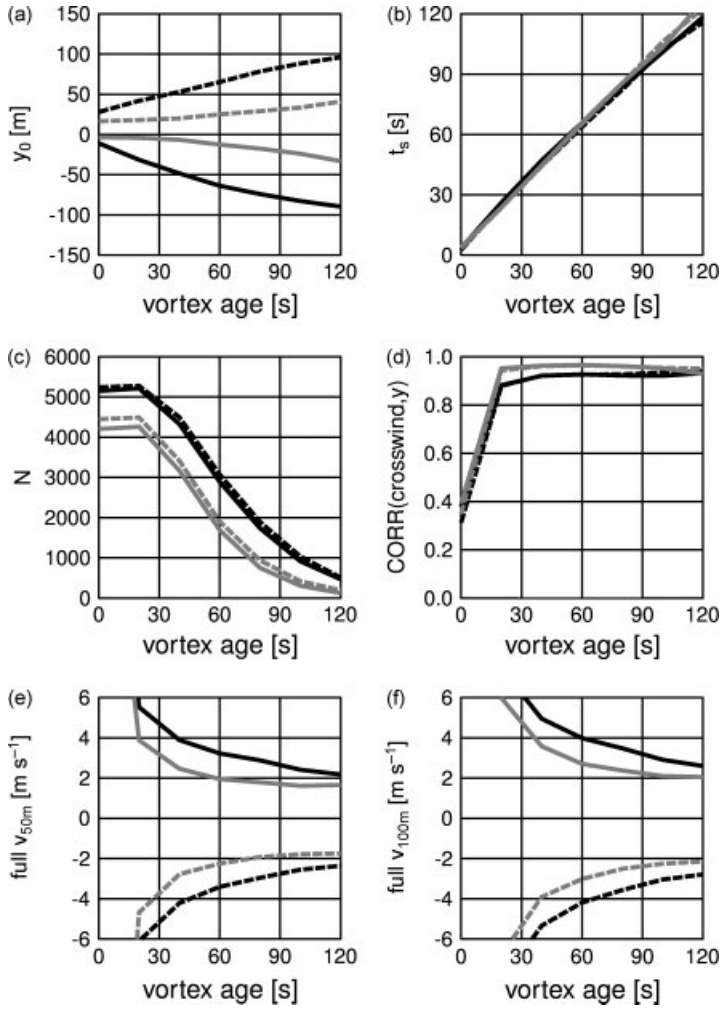

Figure 10. Parameters characterizing the relation between lateral vortex transport and crosswind measured by Lidar in the altitude range where the vortices evolve: (a) offset, (b) slope, (c) number, (d) correlation, (e) 2.5% within ±50 m and (f) 2.5% within ±100 m. Heavy aircraft, left vortex [▬], heavy aircraft, right vortex [▬], medium aircraft, left vortices [▬], right vortices [▬].

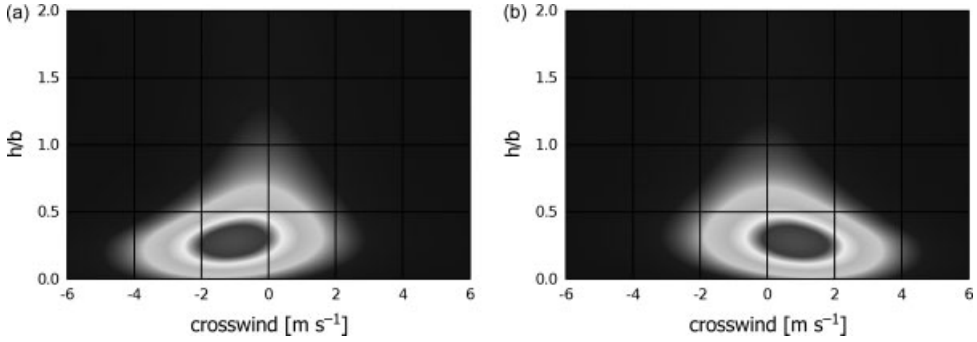

Figure 11. Vortex self induced velocities in ground proximity for heavy aircraft as function of non-dimensional altitude after 60 s of generation: (a) left vortex and (b) right vortex.

vortices towards negative velocities. In addition to that the distributions broaden. Thus, the vicinity to the ground may not be the only factor that determines the self-induced velocities of the vortices. Note that in Figure 11 the wake vortices reach very low altitudes above the ground. This may be related, for example, to the oblate shape of the vortices close to ground. The deteriorated circular symmetry increases the error in the computation of the height of the vortex, because the algorithm assumes a circular shape.

The distributions of altitudes of EDDF-2 heavy and medium aircraft at the intersection with the Lidar scan plane showed that the majority of heavy aircraft wakes is already generated in or near ground effect. In contrast, vortices of medium aircraft were, on average, generated at higher altitudes. If they reach the ground at all they are exposed to ground effect for shorter time before dissipating.

4. Comparison and discussion of the results of the different approaches

Three different ways of analyses have been applied to two different databases resulting in good agreement of the obtained crosswind thresholds. The values of these analyses are summarized in Table V. If not explicitly stated crosswind thresholds for a 60 s separation based on a 95% probability are discussed since for this combination the number of wake vortices within EDDF-1 is high enough to give significant results. The obtained crosswind thresholds lie within 3.5 m s^{-1} (3.9 m s^{-1}) and 4.6 m s^{-1} (5.0 m s^{-1}) for a corridor half width d of 75 m (100 m). In this paragraph possible reasons for the differences in the results obtained will be discussed in more detail.

Table V. Comparison of the crosswind thresholds at 10 m obtained by the different approaches (Nr.).

Nr.	Database	Wind measurement device	d (m)	Clearance time (s)			
				50	60	90	120
1	EDDF-1	Dedicated SONIC	75	4.1	3.7	3.1	2.8
3	EDDF-2	Operational SONIC		–	4.6	–	3.6
2		Lidar		4.0	3.5	2.6	2.2
1	EDDF-1	Dedicated SONIC	100	4.8	4.3	3.5	3.1
3	EDDF-2	Operational SONIC		–	5.0	–	3.8
2		Lidar		–	3.9	2.9	2.4

Distance from the centreline is denoted by d. In all cases a 95% probability is assumed. The SONIC used in the EDDF-1 dataset is denoted as dedicated SONIC.

4.1. Comparison of EDDF-1 (approach 1) and EDDF-2 (approaches 2 and 3)

The crosswind thresholds obtained by using the crosswind measured at 10 m height by the Lidar are generally lower than those obtained by using crosswind at 10 m with standard instrumentation regardless of the used database. As can be seen in Table V this is observed for both corridor widths used in the analysis. This is related to the fact that the wind and wake vortex measurements are conducted in the same measurement plane: that is, the effect of spatial variations of the wind are reduced in this approach. The best correlation between wind and wake vortex transport is achieved when the Lidar data in the height range where the vortices evolve are used.

Another difference of the two campaigns is that in EDDF-2 the Lidar was looking at vortices of heavy aircraft near their rotation point and a large part of the vortices developed in ground proximity. In the EDDF-1 campaign the wake vortices were generated at altitudes of two to eight times of the initial vortex separation. When approaching the ground the wake vortices diverge such that crosswind transport and vortex induced lateral transport overlap. As a consequence a stronger crosswind is needed to transport the luff vortex out of the safety corridor.

In EDDF-1, however, the deviation of the aircraft from the centre line is more pronounced and the deviation between the wind measured at 10 m altitude and the wind sensed by the vortices may be higher, since they are further away from the ground. All these effects are superimposed and may compensate in parts such that the resulting crosswinds in approaches 1 and 2 are similar.

4.2. Comparison between approaches 2 and 3

The reason for the differences observed in the analysis by using the same database EDDF-2 are mainly due to the differences in the way crosswind has been determined. Indeed, using comparable wind measurements, both approaches lead to similar crosswind thresholds. Using the 'filtered in-plane wind' (i.e. the average in-plane wind as measured by the WindTracer, but restricted to the altitude range where the vortices evolved), following approach 3, the crosswind threshold for a corridor half-width of 75 m lies between 4.0 and 4.5 m s^{-1}, for $t_{sep} = 60$ s and between 2.5 and 3.0 m s^{-1}, for $t_{sep} = 120$ s. Following approach 2, when using the crosswind measured by Lidar at the mean altitude of the wake vortices $u_c(h_{mean})$, the obtained threshold is 4.2 m s^{-1}, for $t_{sep} = 60$ s and 2.5 m s^{-1}, for $t_{sep} = 120$ s.

On the other hand, 10 m wind measurements derived from in-plane Lidar measurements (Table III) yield smaller crosswind thresholds than surface winds collected at remote anemometers (Table IV). The potential application of a crosswind-based wake vortex system would require careful selection of the location of wind measurement sites in order to minimize spatial deviations between the measured winds and the winds that actually advect the vortices out of the safety corridor.

4.3. Statistical approach for vortex drift prediction

It can now be assumed that reasonable crosswind thresholds have been obtained using one of the methods described above. A statistical analysis of crosswind changes within a certain time interval Δt could then yield the respective standard deviation of crosswind changes. If the crosswind measured at 10 m height is available every time interval, Δt, the standard deviation of the crosswind change can be deduced statistically. Adding/subtracting multiples of this standard deviation give a probabilistic envelope around the measured crosswind within which the crosswind is expected to be at the end of the defined time interval Δt (Figure 12).

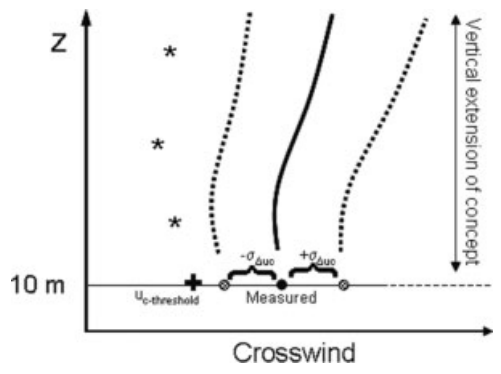

Figure 12. Schematic illustration of a statistical approach for vortex drift prediction. Along the 10 m height level the concept described in the present work is shown with the crosswind threshold, $u_{c-threshold}$ (+) needed, the measured crosswind at a certain time (solid dot) and the standard deviation of the crosswind change, $\sigma_{\Delta uc}$ (shaded dots). Above 10 m altitude a possible extension of the concept is indicated which can be used if vertical wind profiles are available or can be statistically deduced.

Including the crosswind threshold at 10 m height in Figure 12 it can be read as follows. As soon as a new crosswind value is available the standard deviations of crosswind change will be added (subtracted) to give the probabilistic envelope within which the crosswind is expected to be. If this area lies above the crosswind threshold the vortices have travelled a sufficient distance (probability depends on the sigma level used). This idea can be extended vertically provided that crosswind profile measurements are available (solid line shown at higher levels in Figure 12). Such a chart would also show if measured crosswinds at higher levels fall below the threshold values.

5. Conclusions

Two different datasets gathered at Frankfurt airport have been used to estimate crosswind thresholds in order to clear a corridor from wake vortices of departing aircraft. One given data set represents wake vortex evolution in ground proximity whereas the other data set provides wake behaviour at altitudes of up to 400 m above ground. Three different approaches with different assumptions have been applied, leading finally to similar crosswind thresholds. This is remarkable because several competing effects have been identified in the different conducted studies that influence crosswind transport of the wake vortices. These effects comprise wake vortex transport in and out of ground effect, variability of the wind in time and space and the spreading of aircraft trajectories after take-off. It appears that the vortex induced lateral transport of the luff vortex in ground proximity adds up to the lateral spreading of the vortices similarly as the lateral flight path deviations of aircraft out of ground effect and the increased variability of the crosswind at higher altitudes. To reduce the ICAO aircraft separation times of 120 to 60 s a minimum crosswind measured by standard instrumentation at 10 m height between 3.9 and 5.0 m s^{-1} (3.5 and 4.6 m s^{-1}) would be needed to clear a safety corridor of 200 m (150 m) width from wake vortices based on a 95% probability.

The best correlation between wind and wake vortex transport is achieved when the wind is measured close to the air mass in which the vortices actually evolve. For example, the use of a crosswind averaged over the first 100 m height allows more accurate estimations of wake vortex transport and can be obtained from appropriate wind measurement devices. The potential application of a crosswind-based wake vortex system requires careful selection of the location of wind measurement sites in order to minimize spatial deviations between the measured winds and the winds that actually advect the vortices out of the safety corridor.

Complementary to the described analysis crosswind thresholds have been estimated from Monte-Carlo simulations. The Wake Vortex Scenarios Simulation Package

(WakeScene-D) (Holzäpfel *et al*., 2009; Holzäpfel and Kladetzke, 2011) estimates the probability of encountering wake vortices in different traffic and weather scenarios in a domain ranging from the runway to an altitude of 3000 ft (∼914 m) above ground. A combined assessment of vortex encounters regarding frequencies of vortex circulation and distance to the vortex indicates that departure separations of 60 s could be safe for a crosswind threshold of eight knots (4.1 m s^{-1}) at 10 m height. This result confirms the estimations obtained from the pure data analysis. A comprehensive discussion can be found in Holzäpfel and Kladetzke (2009).

The results presented here demonstrate that there is not a simple answer to the question about a definite crosswind threshold. This important quantity is related to other variables, such as the width of the safety corridor which needs to be protected, the required level of probability, the desired aircraft separation time and the location and type of the employed wind measurement device. Further, the question of how the reduced risk of encountering a vortex under favourable crosswind conditions is balanced by the reduced time for vortex decay is not addressed. Nevertheless, the crosswind thresholds obtained from the data analysis confirm the results of Monte Carlo Simulations of the air traffic and the related wake vortex transport and decay and suggest the applicability of a crosswind criterion for reduced departure separations. Safety requirements and risk analyses which assure that a reduced separation does not compromise safety or increase risk are a different part of the EU-project CREDOS and the follow-on project CROPS and are out of the scope of this work.

Acknowledgements

We gratefully acknowledge Fraport AG and METEK GmbH for their support during the measurement campaigns. The authors thank Jean-Pierre Nicolaon from the National Institute of Aerospace for his comments on specific issues. The financial support from the EU project CREDOS (AST5-CT-2006-030837) is greatly acknowledged.

References

Crow SC. 1970. Stability theory for a pair of trailing vortices. *AIAA Journal* **8**: 2172–2179.

De Visscher I, Bricteux L, Karampelas S, Winckelmans G, Holzäpfel F, Baumann R, Roblin Y, Schröder K. 2009. *EDDF-2 Database Analysis and Performance Assessment of the Wake Vortex Models on the EDDF-1 and EDDF-2 Databases*. CREDOS research project D 2-5. Université Catholique de Louvain (UCL): DLR and Airbus-D: Louvain-la-Neuve, Belgium.

Elsenaar B. 2006. *Wake Vortex Research Needs for "Improved Wake Vortex Separation Ruling" and "Reduced Wake Signatures"*. Final Report of the Thematic Network 'WakeNet2-Europe', 6th Framework Programme, NLR-CR-2006-171. National Aerospace Laboratory: Amsterdam, The Netherlands.

Eurocontrol. 2008. Challenges to growth. EATMP Infocentre Eurocontrol Tech. Rep.: 2 pp.

Frech M, Zinner T. 2004. Concept of wake vortex behaviour classes. *Journal of Aircraft* **41**: 564–570.

Hennemann I. 2009. Dreidimensionale verformung und zerfall von flugzeugwirbelschleppen in turbulenter und stabil geschichteter atmosphäre, Dissertation, Deutsches Zentrum für Luft- und Raumfahrt, Oberpfaffenhofen, Germany.

Holzäpfel F. 2003. Probabilistic two-phase wake vortex decay and transport model. *Journal of Aircraft* **40**: 323–331.

Holzäpfel F, Kladetzke J. 2009. Wake vortex encounters during Take-off & departure: sensitivity analysis and worst case search. CREDOS D3-9, 5 November 2009; 94 pp.

Holzäpfel F, Kladetzke J. 2011. Assessment of wake vortex encounter probabilities for crosswind departure scenarios. *Journal of Aircraft* (accepted).

Holzäpfel F, Kladetzke J, Amelsberg S, Lenz H, Schwarz C, De Visscher I. 2009. Aircraft wake vortex scenarios simulation package for takeoff and departure. *Journal of Aircraft* **46**: 713–717.

Holzäpfel F, Steen M. 2007. Aircraft wake-vortex evolution in ground proximity: analysis and parameterization. *AIAA Journal* **45**: 218–227.

ICAO Annex 3. 2004. *Annex 3 to the Convention on International Civil Aviation, Meteorological Service for International Air Navigation Part I Core SARPs and Part II Appendices and Attachments*, 15th edn. November 25, 2004. Montreal, Canada.

Konopka J, Fischer H. 2005. The wake vortex warning system at Frankfurt Airport *Proceedings of the 24th Digital Avionics Systems Conference*, Washington, DC, IEEE, vol. 3; A.6-31–A.6-14.

Konopka J, Fischer H. 2007. *EDDF 6-Month Wake and Weather Dataset RWY25L/R [EDDF-2]*. CREDOS research project D1-2. DFS Deutsche Flugsicherung GmbH: Langen, Germany.

Konopka J, Fischer H. 2008. *EDDF-2 Data Collection Campaign Report*. CREDOS research project D2-4. DFS Deutsche Flugsicherung GmbH: Langen, Germany.

Köpp F, Rahm S, Smalikho I. 2004. Characterization of Aircraft wake vortices by 2-μm pulsed Doppler Lidar. *Journal of Atmospheric and Oceanic Technology* **21**: 194–206.

Köpp F, Rahm S, Smalikoh S, Dolfi A, Cariou JP, Harris M, Young RI. 2005. Comparison of wake-vortex parameters measured by pulsed and continuous-wave Lidars. *Journal of Aircraft* **42**(4): 916–923.

Meleshko VV, Gurzhi AA, Dörnbrack A, Gerz T, Holzäpfel F, Hofbauer T. 2001. Interaction of two-dimensional trailing vortex pair with a shear layer. *International Applied Mechanics* **37**(7): 948–957.

Rossow VJ, Hardy GH, Meyn LA. 2005. Models of wake-vortex spreading mechanisms and their estimated uncertainties. AIAA Paper No. 2005-7353.

Schwarz C, Hahn KU. 2006. Full-flight simulator study for wake vortex hazard area investigation. *Aerospace Science and Technology* **10**(2): 136–143.

Winckelmans G, Cocle R, Dufresne L, Capart R, Bricteux L, Daeninck G, Lonfils T, Duponcheel M, Desenfans O, George L. 2006. Direct numerical simulation and large-eddy simulation of wake vortices: going from laboratory conditions to flight conditions. In *Proceedings of European Conference on Computational Fluid Dynamics (ECCOMAS CFD), Special Technology Session on Wake Vortex Research in Europe, Egmond aan Zee, The Netherlands, 5–8 September 2006*, Wesseling P, Onate E, Périaux J (eds). TU: Delft, The Netherlands.

